DOI: 10.1002/ejic.200800533

Copper(II) Complexes of *N*-Methylated Derivatives of *ortho*- and *meta*-Xylyl-Bridged Bis(1,4,7-triazacyclononane) Ligands: Synthesis, X-ray Structure and Reactivity as Artificial Nucleases

Matthew J. Belousoff,[a] Bim Graham,*[a][‡] and Leone Spiccia*[a]

Dedicated in honour of Professor Jan Reedijk on the occasion of his retirement

Keywords: Copper(II) coordination chemistry / Dinuclear complexes / Macrocyclic ligands / Crystallography / Phosphate ester hydrolysis

Two new binucleating ligands, 1,3-bis[(4,7-dimethyl-1,4,7-triazacyclononan-1-yl)methyl]benzene (L^{memx}) and 1,2-bis[(4,7-dimethyl-1,4,7-triazacyclononan-1-yl)methyl]benzene (L^{meox}), have been prepared from 1,4,7-triazatricyclo[5.2.1.0^{4,10}]decane and applied in the synthesis of the corresponding copper(II) complexes, $[Cu_2(\mu\text{-}AcO)_2(L^{memx})](ClO_4)_2 \cdot H_2O$ (**C$_m$**) and $[Cu_2(\eta_2\text{-}AcO)_2(L^{meox})](ClO_4)_2$ (**C$_o$**). The X-ray crystal structures confirmed the dinuclear nature of the complexes, with pairs of copper(II) centres residing in distorted square-pyramidal coordination environments. The nitrogen donors on the ligands occupy three facially disposed coordination sites about each copper(II) centre, with two acetate ligands completing the copper(II) coordination spheres. For **C$_m$**, both acetate groups bridge the two metal centres, whilst in **C$_o$** each acetate chelates to a single metal centre. To assess their utility as simple nuclease mimics, the metal complexes were tested for their phosphate ester cleavage ability using the model phosphodiester, bis(4-nitrophenyl)phosphate (BNPP). It was found that **C$_o$** exhibited the fastest rate of BNPP hydrolysis ($k_{obsd.} = 2.4 \times 10^{-5}$ s^{-1}), this rate being five times faster than that of the Cu^{II} complex of the non-methylated analogue.

Introduction

A significant area of research in coordination chemistry has been the design and synthesis of metal complexes as low-molecular-weight mimics of the active sites of nuclease and phosphatase metallo-enzymes. These studies have sought to improve our knowledge of how these enzymes function as well as lend understanding to basic metal ion reactivity. The development of complexes as "artificial nucleases" has also been spurred on by the possibility of producing novel therapeutics that not only bind to targeted DNA/RNA sequences, but also cleave the phosphate ester bonds present within the sugar-phosphate backbones, rendering them inactive.[1–4] Complexes of ligands derived from the small, facially coordinating macrocycle, 1,4,7-triazacyclononane (tacn), have featured prominently in these studies. Tacn-derived complexes have been prepared that efficiently cleave model phosphate esters, RNA, DNA and peptides.[3,5–10] One notable finding has been that *N*-alkylation of the tacn ring produces copper(II) complexes that exhibit faster rates of phosphate ester cleavage. This has been attributed in part to a reduced tendency for these complexes to form hydrolytically inactive, hydroxo-bridged dimeric species in solution.[11]

Many hydrolase enzymes contain more than one metal centre at their active site,[12–16] which has led to efforts to prepare dinuclear (and higher nuclearity) model complexes that are able to mimic the synergistic action of the multiple metal centres in these natural systems. Towards this end, multi-macrocyclic ligand assemblies have been used to synthesise polynuclear complexes that exhibit enhanced rates of phosphate ester hydrolysis relative to mononuclear tacn complexes. For example, Morrow and co-workers have reported increases in hydrolytic activity for Zn^{II} complexes of bis(tacn) ligands compared to mononuclear Zn^{II}-tacn complexes.[17–19] Our own studies have shown that the dinuclear copper(II) complexes of xylyl-bridged bis(tacn) ligands are active as phosphate ester cleavage agents.[20] However, these systems were not as active as anticipated, possibly due to their conversion into hydrolytically inactive species in solution.[5,7]

[a] School of Chemistry, Monash University,
Victoria, 3800, Australia
Fax: +61-3-9905-4597
E-mail: leone.spiccia@sci.monash.edu.au
[‡] Current address: Medicinal Chemistry and Drug Action, Monash Institute of Pharmaceutical Sciences, Monash University (Parkville campus),
Victoria, 3052, Australia
Fax: +61-3-9903-9582
E-mail: bim.graham@vcp.monash.edu.au

We now report on our efforts to enhance the activities of these types of complexes through *N*-alkylation of the supporting xylyl-bridged bis(tacn) ligand structures. It was envisaged that this simple modification would sterically hinder the formation of hydroxo-bridged dinuclear complexes and/or mononuclear sandwich-type structures, thus leading to higher effective concentrations of hydrolytically active species in solution. Methylated derivatives of two bis(tacn) ligands, 1,3- and 1,2-bis[(1,4,7-triazacyclononan-1-yl)-methyl]benzene (L^{mx} and L^{ox}),[21] have been synthesised (L^{memx} and L^{meox}) and used in the preparation of two new Cu^{II} complexes, $[Cu_2(\mu\text{-}AcO)_2(L^{memx})](ClO_4)_2\cdot H_2O$ (**C_m**) and $[Cu_2(\eta_2\text{-}AcO)_2(L^{meox})](ClO_4)_2$ (**C_o**). The ability of the complexes to cleave phosphate ester bonds was probed using the well-studied model phosphodiester, bis(4-nitrophenyl)phosphate (BNPP),[7,17,18,22–24] and the results compared to those obtained for previously reported complexes.

Results and Discussion

Synthesis

The methylated ligands (L^{memx} and L^{meox}) were prepared by modifications to the route first described by Farrugia et al.[21] to prepare the two parent bis(macrocycles), L^{mx} and L^{ox}, as their hydrobromide salts. Two equivalents of 1,4,7-triazatricyclo[5.2.0^{4,10}]decane were treated with one equivalent of 1,3-bis(bromomethyl)benzene or 1,2-bis(bromomethyl)benzene to yield bis(amidimium) salt intermediates (see Scheme 1). Hydrolysis and *N*-methylation of these salts was carried out by heating them in a 1:1 mixture of formic acid and aqueous formaldehyde. The fully *N*-methylated ligands were then isolated as their hexahydrochloride salts.

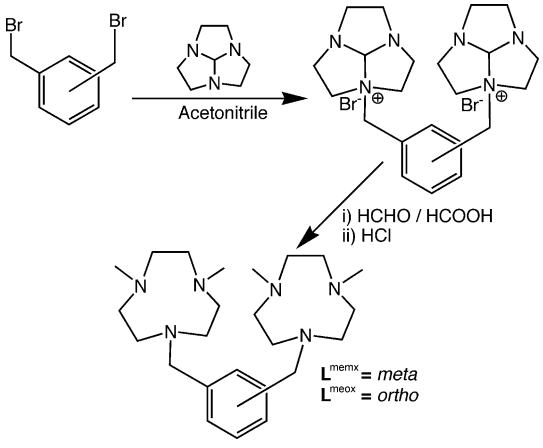

Scheme 1. Synthesis of the ligands.

Spectroscopic analysis of the ligands confirmed their formation. Both the L^{memx} and L^{meox} salts showed *m*/*z* peaks in their electrospray mass spectra at 209.2 and 417.3, corresponding to $[M + 2H]^{2+}$ and $[M + H]^+$, respectively. The ^1H NMR spectra revealed the signals expected for the *ortho*- and *meta*-substituted aromatic rings, as well as a singlet around 3.0 ppm in each case for the four equivalent methyl groups, and a series of signals between ca. 3.2 and 3.8 ppm for the methylene groups of the tacn rings. The xylyl methylenes produced singlets at δ = 4.20 and 4.28 ppm for L^{memx} and L^{meox}, respectively.

The copper(II) complexes, $[Cu_2(\mu\text{-}AcO)_2(L^{memx})](ClO_4)_2\cdot H_2O$ (**C_m**) and $[Cu_2(\eta_2\text{-}AcO)_2(L^{meox})](ClO_4)_2$ (**C_o**), were formed by reacting the ligands L^{meox} and L^{memx} (as HCl salts) with one equiv. of cupric perchlorate and one equiv. of cupric acetate at pH 7.0. Satisfactory C H N microanalyses were obtained for both complexes, and IR spectroscopy confirmed the presence of the acetate groups. The υ_{asym} carboxylate stretches were observed at 1572 and 1560 cm^{-1} for **C_m** and **C_o**, respectively.[25,26] In each case, the υ_{sym} stretch was difficult to assign due to the presence of $\upsilon_{C=C}$ stretches in the 1400–1600 cm^{-1} region. The UV/Vis spectra showed a weak d→d transition at 668 nm, consistent with square-pyramidal or distorted octahedral Cu^{II} coordination geometry,[27] and a strong band at 274 nm due to ligand π→π* transitions.

Crystallography

The X-ray crystal structure of **C_m** confirmed the formation of a dinuclear copper(II) complex with the formula, $[Cu_2(\mu\text{-}AcO)_2(L^{memx})](ClO_4)_2\cdot H_2O$. A representation of the cationic unit is shown in Figure 1, with selected bonds lengths and angles given in Table 1. Three of the five coordination sites about each copper(II) centre are occupied by the nitrogen atoms of a facially coordinating tacn macrocycle, and the other two by the oxygen atoms of two acetate groups that bridge between the two centres. Both copper centres exist in square-pyramidal coordination spheres, with the Cu(1)–N(3) and Cu(2)–N(6) distances being > 0.1 Å longer than the Cu–N distances in the basal plane. The square-pyramidal geometry is distorted (with an Addison[28] parameter of τ = 0.16; note that τ = 0 for ideal square-pyramidal geometry and τ = 1 for trigonal-bipyramidal geometry), due mainly to the constraints imposed by the tridentate coordination of the strained tacn macrocycles, forcing the N–Cu–N angles all below the ideal 90°. For each copper centre, the two Cu–O distances to the bridging acetates differ by 0.051(4) Å and 0.029(4) Å for Cu(1)–O(1A)/Cu(1)–O(3A) and Cu(2)–O(2A)/Cu(2)–O(4A), respectively.

Unlike many other copper(II) tacn-based complexes, there is no weakly interacting solvent or counterion molecule in proximity to the sixth, "vacant" coordination site. Instead, a xylyl hydrogen, H(24), is in close proximity, but not within bonding distance to the copper centres [Cu···H(24) = 2.397(1) and 2.651 Å for Cu(1) and Cu(2), respectively; see Figure 1].

The bridging acetate groups in **C_m** result in a Cu···Cu separation of 3.874(3) Å, compared to distances of ca. 2.9 Å found for structures featuring dihydroxo-bridged copper(II) centres.[21,29] A least-squares plane analysis shows that the angle between the planes of the acetate groups and the basal coordination plane of Cu(1) are 61.29(2)° and

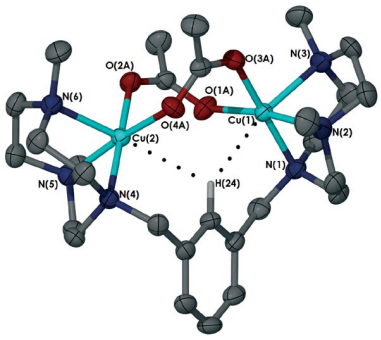

Figure 1. Thermal ellipsoid plot of the complex cation in $\mathbf{C_m}$ [thermal ellipsoids drawn at 50%; selected hydrogen atoms omitted for clarity; dotted line indicates a close, non-bonding interaction with H(24)].

Table 1. Selected bond lengths and angles for $\mathbf{C_m}$.

	Distance [Å]		Angle [°]
Cu(1)···Cu(2)	3.874(3)	O(3A)–Cu(1)–O(1A)	92.15(1)
Cu(1)–O(3A)	1.935(3)	O(1A)–Cu(1)–N(1)	90.27(1)
Cu(1)–O(1A)	1.986(3)	O(3A)–Cu(1)–N(2)	92.02(1)
Cu(1)–N(1)	2.041(3)	N(1)–Cu(1)–N(2)	85.44(1)
Cu(1)–N(2)	2.082(3)	O(3A)–Cu(1)–N(3)	95.95(1)
Cu(1)–N(3)	2.204(3)	N(1)–Cu(1)–N(3)	84.66(1)
Cu(2)–O(2A)	1.955(3)	N(2)–Cu(1)–N(3)	84.85(2)
Cu(2)–O(4A)	1.984(3)	O(3A)–Cu(1)–O(1A)	92.15(1)
Cu(2)–N(4)	2.065(3)	O(1A)–Cu(1)–N(1)	90.27(1)
Cu(2)–N(5)	2.074(3)	O(3A)–Cu(1)–N(2)	92.02(1)
Cu(2)–N(6)	2.213(3)	N(1)–Cu(1)–N(2)	85.44(1)
		O(3A)–Cu(1)–N(3)	95.95(1)
		N(1)–Cu(1)–N(3)	84.66(1)
		N(2)–Cu(1)–N(3)	84.85(2)

78.14(2)°, and 75.67(3)° and 61.29(2)° for the basal plane of Cu(2). Thus, the $Cu_2(\mu_2\text{-ac})_2$ motif possesses pseudo-C_2 symmetry. This motif is rare amongst the various binding motifs that have been reported in the literature for copper(II)-acetato complexes (see Figure 2). Tokii et al.[30] reported the same binding mode in a copper(II) complexes with 1,10-phenanthroline ligands. Their reported Cu···Cu separation of 3.063(3) Å is much shorter than that found in $\mathbf{C_m}$ due to the π–π interaction between the chelating phen ligands on the two copper centres forming the dinuclear complex. This causes the acetate bridge to bend, bringing the two copper centres in closer proximity. The most common bridging motif observed in copper(II)-acetato complexes is the $Cu_2(\mu_2\text{-ac})_4$ unit, where four acetate ligands bridge between two copper(II) centres, usually resulting in C_4 symmetry about the copper centres and closer Cu···Cu distances of around 2.5 Å.[31] Structurally similar molecules to $\mathbf{C_m}$ but which have a $Cu_2(\mu_2\text{-ac})(\mu\text{-O})$ binding motif show Cu···Cu distances around 3.3–3.6 Å.[32–36] These compounds show promise as catalysts for catechol oxidation,[32,36] and also as model systems for the tyrosinase active site.[34] The $\mathbf{C_m}$ complex has some structural similarities to the active site of the hydrolase enzyme, methane mono-oxygenase,[37–42] which features a dicarboxalato-bridged diiron core, but with an additional water-derived ligand bridging the two iron(III) centres.[40] There is a membrane-bound form of this enzyme found in the bacteria *Methylococcus capsulatus* (Bath), which has not been characterized by X-ray crystallography, but which is believed to use a mixed-metal (copper/iron) active site to carry out electron-transfer reactions, and the complex $\mathbf{C_m}$ could be a relevant structural mimic for this enzyme.

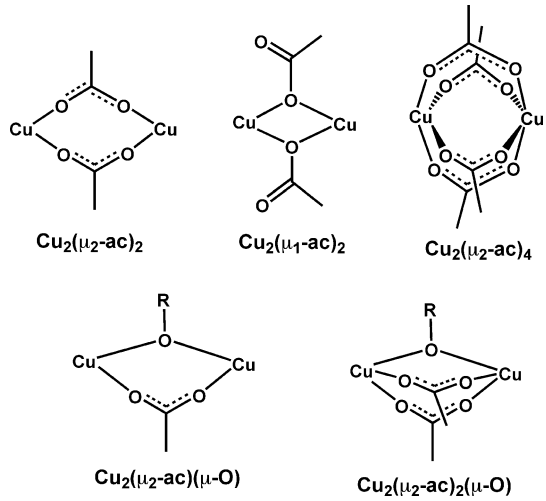

Figure 2. Bridging motifs found in Cu^{II} acetate dimers.

The X-ray crystal structure of $\mathbf{C_o}$, $[Cu_2(\eta_2\text{-AcO})_2(L^{meox})](ClO_4)_2$, revealed the presence of a dinuclear copper(II) complex cation (see Figure 3; selected bond lengths and angles given in Table 2), in which the two tacn macrocycles of the ligand lie on opposite sides of the plane of the central aromatic ring. Thus, the complex adopts an *anti* configuration, placing the two copper centres 6.578(4) Å away from each other, nearly twice the Cu···Cu distance observed in $\mathbf{C_m}$. The complex is pseudo-C_2 symmetric about an axis bisecting the *o*-xylyl bridge, and its general structural form resembles that of a copper(II) complex of the non-alkylated parent ligand, L^{ox}, reported by Graham et al.[43] In $\mathbf{C_o}$, however, bidentate acetate ligands replace the monodentate bromide ligands in $[Cu_2(L^{ox})Br_4]$. In contrast to $\mathbf{C_m}$, the two acetate ligands in $\mathbf{C_o}$ chelate to either Cu(1) or Cu(2), forming constricted, three-membered chelate rings, with O–Cu–O angles of 65.23(2) and 65.57(2)° for Cu(1) and Cu(2), respectively. The chelating acetates do not bind symmetrically to Cu(2), viz., a difference in the two Cu–O bond lengths of 0.071(4) Å for Cu(2)–O(11)/O(12), cf., 0.005(4) Å

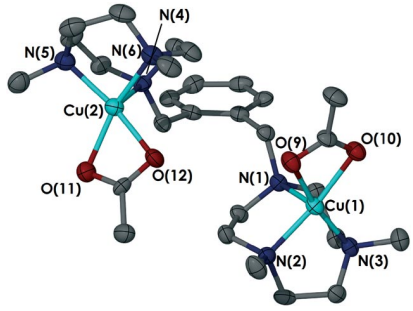

Figure 3. Thermal ellipsoid plot of the complex cation in $\mathbf{C_o}$ (thermal ellipsoids drawn at 50%; hydrogen atoms omitted for clarity).

for Cu(1)–O(9)/O(10). This asymmetry in acetate binding to Cu(2) may be due to the slightly weaker interaction of the Cu(2) with the perchlorate anion (vide infra). As for $\mathbf{C_m}$, the Cu–N_{eq} distances are significantly shorter (by > 0.2 Å) than the Cu–N_{ax} distances.

As a consequence of the arrangement of the nitrogen and oxygen donors, the geometry of the metal centre is once again distorted from ideal square pyramidal, with the angles in the basal plane of the pyramid all greatly deviating from the ideal 90° (see Table 2). This is evident from the value of the geometric parameter, $\tau = 0.20$.[28]

The copper(II) centres in $\mathbf{C_o}$ participate in very weak interactions with the perchlorate anions (Figure 4), two of which weakly bridge between two adjacent complex cation units [Cu–O (perchlorate): 2.951(4) Å and 2.822(3) Å] forming a head-to-head arrangement.

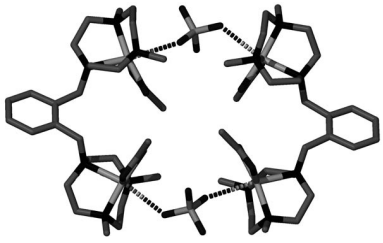

Figure 4. Stick representation showing bridging of two complex cations in $\mathbf{C_o}$ by two weakly binding perchlorate anions (hydrogen atoms and other counterions omitted for clarity).

Table 2. Selected bond lengths and angles for $\mathbf{C_o}$.

	Distance [Å]		Angle [°]
Cu(1)–Cu(2)	6.578(4)	N(3)–Cu(1)–N(2)	86.6(2)
Cu(1)–N(1)	2.259(5)	N(3)–Cu(1)–N(1)	84.76(2)
Cu(1)–N(3)	2.001(5)	N(2)–Cu(1)–N(1)	84.71(2)
Cu(1)–N(2)	2.012(5)	O(9)–Cu(1)–O(10)	65.57(2)
Cu(1)–O(9)	2.013(4)	N(3)–Cu(1)–O(9)	169.24(2)
Cu(1)–O(10)	2.018(4)	N(2)–Cu(1)–O(9)	101.43(2)
Cu(2)–N(4)	2.240(5)	N(3)–Cu(1)–O(10)	105.88(2)
Cu(2)–N(5)	1.994(5)	N(2)–Cu(1)–O(10)	166.57(2)
Cu(2)–N(6)	2.019(5)	O(9)–Cu(1)–N(1)	102.95(2)
Cu(2)–O(12)	1.986(4)	O(10)–Cu(1)–N(1)	101.08(2)
Cu(2)–O(11)	2.057(4)	N(5)–Cu(2)–N(4)	84.65(2)
		N(6)–Cu(2)–N(4)	85.36(2)
		N(5)–Cu(2)–N(6)	87.9(2)
		O(12)–Cu(2)–O(11)	65.23(2)
		N(5)–Cu(2)–O(11)	108.2(2)
		N(6)–Cu(2)–O(11)	158.2(2)
		O(12)–Cu(2)–N(4)	106.24(2)
		O(11)–Cu(2)–N(4)	110.07(2)
		O(12)–Cu(2)–N(5)	168.6(2)
		O(12)–Cu(2)–N(6)	96.3(2)

Phosphate Ester Hydrolysis

The ability of the two complexes to hydrolyse phosphate esters was explored by examining their ability to accelerate the cleavage of the model phosphodiester, BNPP, which, upon hydrolysis, liberates a 4-nitrophenolate (NP) anion, a chromophore that adsorbs strongly at 400 nm [i.e. $NO_2PhOP(O)_2OPhNO_2$ (BNPP) + complex → NO_2PhO^- (4-nitrophenolate) + $^-O_3POPhNO_2$ (4-nitrophenylphosphate) + complex]. For this investigation, we used a large excess of complex relative to BNPP (to ensure first-order kinetics) and studied the cleavage at a temperature of 50 °C and near physiological pH (7.4). In the case of $\mathbf{C_o}$, the absorbance-vs.-time data was fitted to an exponential function that yielded the rate constant directly. For the reaction of the $\mathbf{C_m}$ complex with BNPP, the data was fitted using the initial rates method reported by Burstyn et al.[6] The obtained rate constants for $\mathbf{C_o}$ and $\mathbf{C_m}$, as well as a series of related complexes, are listed in Table 3.

Table 3. Rates of reaction of copper complexes with BNPP.[a]

Compound	$k_{obsd.} \times 10^5$ s^{-1}	Ref.
Base-catalysed hydrolysis of BNPP at 100 °C	0.04	[7]
Cu^{II}-tacn[b]	0.025	[7]
Cu^{II}-*i*Pr_3tacn	4.3	[7]
Cu^{II}-Me_3tacn	3.7	[7]
$[Cu_2L^{ox}(H_2O)_4]^{4+}$	0.52	[20][b]
$[Cu_2L^{mx}(H_2O)_4]^{4+}$	0.086	[20][b]
$[Cu_2(\eta\text{-}AcO)_2(L^{meox})](ClO_4)_2$ ($\mathbf{C_o}$)	2.43	this work
$[Cu_2(\mu\text{-}AcO)_2(L^{memx})](ClO_4)_2{\cdot}H_2O$ ($\mathbf{C_m}$)	0.11	this work

[a] Conditions used: [BNPP] = 0.015 mM, [complex] = 1.0 mM, I = 0.15 M ($NaClO_4$), T = 50 °C, pH 7.4 (buffered with MOPS). [b] Conditions used: [BNPP] = 0.15 mM, [complex] = 1.7 mM, pH 7.4 (HEPES), I = 0.15 M ($NaClO_4$), and T = 50 °C. Abbreviations: *i*Pr_3tacn = 1,4,7-tris(isopropyl)-1,4,7-triazacyclononane; Me_3tacn = 1,4,7-trimethyl-1,4,7-triazacyclononane; L^{ox} = 1,2-bis[(1,4,7-triazacyclonon-1-yl)methyl]benzene; L^{mx} = 1,3-bis[(1,4,7-triazacyclonon-1-yl)methyl]benzene.

Previously published data (Table 3) indicated that the two copper(II) centres in the L^{ox} complex exhibit some degree of cooperativity in carrying out the hydrolysis of BNPP, whilst those in the L^{mx} complex act essentially independently, because the rate constants for the dinuclear complexes of L^{ox} and L^{mx} are ca. 21- and threefold higher, respectively, than that of the Cu^{II}-tacn complex. Secondly, alkylation of the tacn ring nitrogen atoms generally leads to rate enhancements. This is most pronounced for the mononuclear complexes, with the Cu^{II} complexes of Me_3tacn and *i*Pr_3tacn exhibiting rate constants 150- and 170-times higher, respectively, than the Cu^{II}-tacn complex. Comparison of the rate constants for $\mathbf{C_o}$ (the complex of the methylated L^{ox} ligand) and the dinuclear copper(II) complex of L^{ox} indicate that simple *N*-methylation of the supporting ligand structure results in a fivefold increase in rate constant, while for the *m*-xylyl-bridged ligand, L^{mx}, *N*-methylation results in only a very slight increase in rate.

One reason that has been suggested for the higher rate constants for the Cu^{II} complexes of Me_3tacn and *i*Pr_3tacn relative to the Cu^{II}-tacn complex is that the alkyl groups hinder dimerisation of mononuclear cation units into a hydrolytically inactive, dihydroxo-bridged dinuclear complex, or conversion into sandwich complexes of the form $[L_2Cu]^{2+}$, which no longer have sites available for the attachment of the substrate or the aqua ligands required to generate the coordinated nucleophile to attack the substrate. These factors are also probably responsible for the enhanced rate constants of the dinuclear complexes of

L^{meox} and L^{memx} relative to those of L^{ox} and L^{mx}, respectively. However, in the case of the dinuclear complexes, the effects of methylation on rate constant are not as impressive as for the simple monuclear complexes, as can be seen in Table 3.

For the *m*-xylyl-bridged ligands, L^{mx} and L^{memx}, it would appear that the ligand geometry is particularly suited to intramolecular dihydroxo-bridge formation between copper(II) centres. Indeed, the intramolecular dihydroxo-bridged dinuclear copper(II) complex of L^{mx} has been isolated by Farrugia et al.,[21] and we have structurally characterised several copper(II) complexes of ligands featuring pairs of dihydroxo-bridged Cu^{II}-tacn units attached to the *meta* positions of an aromatic ring.[44] Thus, at pH 7.4, significant proportions of the dinuclear Cu^{II} complexes of L^{mx} and L^{memx} could be present as intramolecular hydroxo-bridged dimers, substantially lowering the effective concentration of hydrolytically active species in solution. The similarity in the rate constant for hydrolysis of BNPP by the complexes of L^{mx} and L^{memx} to that for the tacn complex appears to bear this point out.

The data for the copper(II) complexes of the *o*-xylyl-bridged ligands, L^{ox} and L^{meox}, indicate that *N*-methylation translates into a much more significant (5-fold) increase in rate constant than for the *m*-xylyl-bridged systems, suggesting that alkylation of the secondary amines serves to more effectively hinder the formation of hydrolytically inactive species in solution in this case. This may be related to the fact that the *o*-xylyl bridge is already less accommodating of intramolecular dihydroxo-bridge formation between the two copper(II) centres than the *m*-xylyl bridge (Zompa and co-workers[45] have reported the $\log\beta$ for formation of the intramolecular hydroxo-briged dinuclear copper complex of L^{mx} to be higher than that of L^{ox}). Nonetheless, the fact that the rate constant for $\mathbf{C_o}$ is *not* significantly higher than that of the Cu^{II}-Me_3tacn complex suggests that *N*-methylation is unable to completely suppress intramolecular hydroxo-bridge formation between the proximal Cu^{II} centers in the *o*-xylyl-bridged complex.

It should also be noted that our earlier work,[43] and a subsequent study by Zompa and co-workers,[45] have shown that L^{ox} is capable of forming a stable mononuclear "sandwich complex" with Cu^{2+} ions. Upon dissolution of the dinuclear complex of L^{ox} in aqueous solution, some complex rearrangement may be occurring, leading to formation of less active or inactive complexes, i.e. $[L^{ox}Cu]^{2+}$, $[L^{ox}Cu_2(OH_2)]^{2+}$ and Cu^{2+}. The introduction of methyl groups onto the four nitrogen atoms of L^{ox} would be expected to sterically hinder, but not necessarily prevent, the formation of such complexes. The moderate rate enhancement observed in moving from the copper(II) complex of L^{ox} to that of the fully methylated analogue, L^{meox}, may be originating from subtle changes in species distribution.

Conclusion

Two new methylated, xylyl-bridged bis(tacn) ligands L^{meox} and L^{memx} have been prepared, together with their corresponding dinuclear copper(II) complexes, $[Cu_2(\eta\text{-}AcO)_2(L^{meox})](ClO_4)$ and $[Cu_2(\mu\text{-}AcO)_2(L^{memx})](ClO_4)_2\cdot H_2O$. In these complexes, the acetato ligands were found to adopt chelating and bridging coordination modes, respectively, owing to the structural constraints of the *ortho*- and *meta*-substituted xylyl backbone. Methylation of all four nitrogen atoms of the *o*-xylyl-bridged bis(tacn) ligand results in a fivefold increase in the BNPP hydrolysis rate by the corresponding dinuclear copper(II) complex relative to that of the complex of the non-methylated ligand. In contrast, *N*-methylation of the *m*-xylyl-bridged bis(tacn) ligand has little impact on BNPP hydrolysis rates.

Experimental Section

General: All reagents and solvents used were of reagent or analytical grade and were used as received from commercial suppliers. Distilled H_2O was used throughout. Acetonitrile was pre-dried with 4 Å sieves and used without further purification. 1,4,7-Triazatricyclo[5.2.1.$0^{4,10}$]decane was synthesized according to published methods.[46]

Instrumentation and Methods: All NMR spectra were recorded using Bruker spectrometers. ^1H and ^{13}C spectra were performed in D_2O at 25 °C using a 400 MHz instrument. UV/Vis spectra were recorded using Varian Cary 300 or Cary 5G spectrophotometers. IR spectra were recorded using Perkin–Elmer FTIR 1600 series spectrometer at 4.0-cm^{-1} resolution, using KBr discs. Cation-exchange column chromatography was performed using Sephadex™ SP-C25 columns (Na^+ form) with a 30-mm diameter. All mass spectrometry was performed using a Micromass Platform II, with an ESI source. The capillary voltage was at 3.5 eV and the cone voltage at 35 V.

1,3-Bis[(4,7-dimethyl-1,4,7-triazacyclononan-1-yl)methyl]benzene Hexahydrochloride (L^{memx}·6HCl): An acetonitrile solution (5 mL) of 1,3-bis(bromomethyl)benzene (0.284 g, 1.08 mmol) was added to a stirred solution of 1,4,7-triazatricyclo[5.2.1.$0^{4,10}$]decane (0.300 g, 2.16 mmol) in acetonitrile (5 mL) was added dropwise . Once addition was complete, the reaction was stirred at room temperature for 15 h. The resulting white precipitate was filtered, washed with acetonitrile (2 x 3 mL) and diethyl ether (3 × 10 mL), and then dissolved in a 1:1 v/v solution of formic acid and aqueous formaldehyde (40%) (20 mL). The flask was fitted with a reflux condenser and the resulting solution was heated at 70 °C for 20 h. The mixture was then cooled to room temperature and the solvent removed under vacuum. The resulting oil was taken up in 2 M HCl (20 mL) and the solvent again removed under vacuum. Trituration of the oily residue with acetone (10 mL) yielded a white solid corresponding to the acid salt of L^{memx}. This was filtered and washed with acetone (10 mL) and diethyl ether (10 mL). Yield 0.51 g, 74%. ESI-MS: m/z = 209.1889 $[M + 2H]^{2+}$, 417.3695 $[M + H]^+$. ^1H NMR (400 MHz, D_2O): δ = 7.701–7.628 (m, 4 H, aromatic CH), 4.201 (s, 4 H, benzyl CH_2), 3.714 (br., 10 H, tacn ring CH_2), 3.414–3.219 (m, 14 H, tacn ring CH_2), 3.041 (s, 12 H, N-CH_3 ppm) ppm. ^{13}C NMR (300 MHz, D_2O): δ = 132.967, 131.516, 130.276, 56.612, 53.262, 51.782, 48.291, 44.989, 30.758 ppm.

1,2-Bis[(4,7-dimethyl-1,4,7-triazacyclononan-1-yl)methyl]benzene Hexahydrochloride (L^{meox}·6HCl): The product was obtained as a white solid according to the procedure described above for L^{memx}·6HCl, starting from 1,4,7-triazatricyclo[5.2.1.$0^{4,10}$]decane (0.312 g, 2.25 mmol) and 1,2-bis(bromomethyl)benzene (0.295 g,

1.12 mmol). Yield 0.49 g, 69%. ESI-MS: *m*/*z* = 209.1895 [M + 2H]$^{2+}$, 417.3698 [M + H]$^{+}$. ^{1}H NMR (400 MHz, D_2O): δ = 7.7757 (AB quartet, J_1 = 3.56, J_2 = 4.96 Hz, 2 H, aromatic CH), 7.6142 (AB quartet, J_1 = 3.56, J_2 = 4.96 Hz, 2 H, aromatic CH), 4.283 (s, 4 H, benzyl CH_2), 3.8021 (br., 8 H, tacn ring CH_2), 3.4144 (br., 6 H, tacn ring CH_2), 3.2467 (br., 10 H, tacn ring CH_2), 2.9855 (s, 12 H, N-CH_3) ppm. ^{13}C NMR (400 MHz, D_2O): δ = 131.90, 129.53, 62.32, 55.13, 53.24, 51.46, 48.62, 44.49, 30.34 ppm.

[Cu_2(μ-AcO)$_2$(L^{memx})](ClO$_4$)$_2$·H_2O (C_m): Aqueous solutions of Cu(ClO$_4$)$_2$·6H_2O (100 mM, 1 mL) and Cu(ac)$_2$·H_2O (100 mM, 1 mL) were added to an aqueous solution of L^{memx}·6HCl (96 mM, 2 mL). The pH of the resulting solution was adjusted to pH 7.0 with sodium hydroxide, upon which the colour became a deep royal blue. The solution was carefully taken to dryness under vacuum and the resulting solid residue dissolved in acetonitrile and filtered. Diethyl ether was diffused into the filtrate, upon which green crystals formed. Yield 68 mg, 40%. UV/Vis (H_2O): λ_{max} (ε_{max}, M^{-1}cm^{-1}) = 272 (7100), 668 nm (56). IR: $\tilde{\nu}$ = 2924 (s), 2869 (s), 1572 (s), 1492 (w), 1466 (s), 1432 (s), 1420 (s), 1347 (w), 1324 (w), 1292 (w), 1253 (w), 1224 (w), 1090 (br), 1012 (m), 984 (m), 890 (w), 821 (m), 787 (w), 753 (w), 714 (w), 668 (w), 624 (s) cm^{-1}. $C_{28}H_{58}Cl_2Cu_2N_6O_{16}$ (930.8): calcd. C 36.8, H 6.2, N 9.2; found C 36.0, H 5.9, N 9.2.

[Cu_2(η-AcO)$_2$(L^{meox})](ClO$_4$)$_2$ (C_o): Aqueous solutions of Cu(ClO$_4$)$_2$·6H_2O (100 mM, 0.26 mL) and Cu(ac)$_2$·H_2O (100 mM, 0.26 mL) were added to an aqueous solution of L^{meox}·6HCl (120 mM, 0.5 mL). The pH of the resulting solution was adjusted to pH 7.0 with sodium hydroxide, upon which the colour became a deep royal blue. Work-up as described for the synthesis of C_m gave blue crystals of C_o. Yield 36 mg, 69%. UV/Vis (H_2O): λ_{max} (ε_{max}, M^{-1}cm^{-1}) = 274 (7400), 668 nm (68). IR: $\tilde{\nu}$ = 3443 (br), 2927 (m), 2875 (m), 2832 (w), 1560 (m), 1508 (s), 1498 (s), 1460 (s), 1472 (s), 1411 (s), 1331 (m), 1299 (m), 1201 (w), 1095 (br. s), 995 (m), 974 (w), 946 (m), 902 (w), 836 (w), 818 (w), 792 (m), 747 (m), 736 (w), 696 (m), 658 (w), 624 (s) cm^{-1}. $C_{28}H_{50}Cl_2Cu_2N_6O_{12}$ (860.7): calcd. C 39.1, H 5.9, N 9.8; found C 39.1, H 6.0, N 10.3.

Crystals of the complexes suitable for X-ray crystallography were obtained through slow evaporation of solutions of the complexes in 30% acetonitrile/1 M $NaClO_4$.

Phosphate Ester Cleavage Kinetics: These experiments were conducted as described previously.[5,7] Briefly, the rate of cleavage of bis(4-nitrophenyl)phosphate, BNPP, by the Cu^{II} complexes was measured at pH 7.4 (MOPS buffer) and T = 50 °C by following the formation of *p*-nitrophenolate ion (λ_{max} = 400 nm, ε_{max} = 18700 M^{-1}cm^{-1}) in solution containing 15 μM BNPP, 1 mM Cu^{II} complex and I = 0.15 M ($NaClO_4$), with a Varian Cary 300 spectrophotometer. Absorbance measurements were commenced after 2 min and were continued for 8000 min with a reading taken every 5 min. As the complex was in large excess compared to BNPP, the appearance of NP (and cleavage of BNPP) was modelled as a first-order process, Abs = $A + Be^{k_{obsd.}t}$, for C_o, and using the initial rates method for C_m, as per previous studies.[6,7]

Table 4. Crystal collection parameters for C_m·H_2O and C_o.

Crystal	C_m	C_o
Empirical formula	$C_{28}H_{52}Cl_2Cu_2N_6O_{13}$	$C_{28}H_{50}Cl_2Cu_2N_6O_{12}$
M [g mol^{-1}]	878.75	860.72
Crystal system	monoclinic	orthorhombic
Space group	$P2_1/n$	$Pbca$
a [Å]	15.029(3)	15.041(3)
b [Å]	11.507(2)	19.082(4)
c [Å]	21.503(4)	25.166(5)
β [°]	96.00(3)	
Volume [Å^3]	3698.4(13)	7223(2)
Z	4	8
μ (Mo-K_α) [mm^{-1}]	1.364	1.393
D_c [g cm^{-3}]	1.578	1.583
Data measured	90662	66176
Unique data (R_{int})	8495 (0.0820)	8260 (0.1803)
Observed data [$I > 2\sigma I$]	6361	3578
Final R_1[a], wR_2[b] (obsd. data)	0.0539[a], 0.1326[b]	0.0697[a], 0.1363[b]
Final R_1, wR_2 (all data)	0.0868, 0.1729	0.2005, 0.1880
ρ_{min}, ρ_{max} [e Å^3]	–1.238, 0.861	–0.903, 0.700

[a] $R = \Sigma(|F_o| - |F_c|)/\Sigma|F_o|$. [b] $R' = [\Sigma w(|F_o| - |F_c|)^2/\Sigma F_o^2]^{1/2}$, where $w = [\sigma^2(F_o)]^{-1}$.

Crystallography: Intensity data for a green crystal of C_m and a dark blue crystal of C_o were measured at 123 K with a Nonius Kappa CCD fitted with graphite-monochromated Mo-K_α radiation (0.71073 Å). The data were collected to a maximum 2θ value of 55° and processed using the Nonius software. Crystal parameters and details of the data collection are summarised in Table 4. Both structures were solved by direct methods and expanded using standard Fourier routines in the SHELX-97 software package.[47,48] All hydrogen atoms were placed in idealised positions, and all non-hydrogen atoms were refined anisotropically.

CCDC-610106 (for C_m) and -610107 (for C_o) contain the supplementary crystallographic data for this paper. These data can be obtained free of charge from The Cambridge Crystallographic Data Centre via www.ccdc.cam.ac.uk/datarequest/cif.

[1] F. H. Zelder, A. A. Mokhir, R. Kramer, *Inorg. Chem.* **2003**, *42*, 8618–8620.
[2] E. L. Hegg, J. N. Burstyn, *Inorg. Chem.* **1996**, *35*, 7474–7481.
[3] E. L. Hegg, J. N. Burstyn, K. A. Deal, L. L. Kiessling, *Inorg. Chem.* **1997**, *36*, 1715–1718.
[4] E. L. Hegg, J. N. Burstyn, *Coord. Chem. Rev.* **1998**, *173*, 133–165.
[5] M. J. Belousoff, M. B. Duriska, B. Graham, S. R. Batten, B. Moubaraki, K. S. Murray, L. Spiccia, *Inorg. Chem.* **2006**, *45*, 3746.
[6] K. A. Deal, J. N. Burstyn, *Inorg. Chem.* **1996**, *35*, 2792–2798.
[7] F. Fry, A. J. Fischmann, M. J. Belousoff, L. Spiccia, J. Brugger, *Inorg. Chem.* **2005**, *44*, 941.
[8] F. H. Fry, P. Jensen, C. M. Kepert, L. Spiccia, *Inorg. Chem.* **2003**, *42*, 5637.
[9] E. L. Hegg, J. N. Burstyn, *J. Am. Chem. Soc.* **1995**, *117*, 7015–7016.
[10] K. P. McCue, J. R. Morrow, *Inorg. Chem.* **1999**, *38*, 6136–6142.
[11] K. M. Deck, T. A. Tseng, J. N. Burstyn, *Inorg. Chem.* **2002**, *41*, 669–677.
[12] A. Vogel, F. Spener, B. Krebs, *Purple Acid Phosphatase* in *Handbook of Metalloproteins*, vol. 2, p. 752, Wiley, Chichester, **2001**.
[13] E. R. Kantrowitz, *Handbook of Metalloproteins* (Eds.: A. Messerschmidt, W. Bode, M. Cygler), vol. 3, p. 71, Wiley, **2004**,.
[14] E. E. Kim, H. W. Wyckoff, *J. Mol. Biol.* **1991**, *218*, 449.
[15] T. Knofel, N. Strater, *J. Mol. Biol.* **2001**, *309*, 239.
[16] L. W. Guddat, A. S. McAlpine, D. Hume, S. Hamilton, J. Jersey, J. L. Martin, *Structure* **1999**, *7*, 757.
[17] O. Iranzo, J. P. Richard, J. R. Morrow, T. Elmer, *Inorg. Chem.* **2003**, *42*, 7737–7746.
[18] O. Iranzo, J. P. Richard, J. R. Morrow, A. Y. Kovalevsky, *J. Am. Chem. Soc.* **2003**, *125*, 1988–1993.
[19] M.-Y. Yang, J. P. Richard, J. R. Morrow, *Chem. Commun.* **2003**, 2832.
[20] F. Fry, L. Spiccia, P. Jensen, B. Moubaraki, K. Murray, E. R. T. Tiekink, *Inorg. Chem.* **2003**, *42*, 5594–5603.
[21] L. J. Farrugia, P. A. Lovatt, R. D. Peacock, *J. Chem. Soc., Dalton Trans.* **1997**, 911.
[22] E. L. Hegg, S. H. Mortimore, C. L. Cheung, J. E. Huyett, D. R. Powell, J. N. Burstyn, *Inorg. Chem.* **1998**, *38*, 2691–2698.

[23] J. N. Burstyn, K. A. Deal, *Inorg. Chem.* **1993**, *32*, 3585–3586.
[24] C. Vichard, T. A. Kaden, *Inorg. Chim. Acta* **2002**, *337*, 173.
[25] K. Nakamoto, *Infrared and Raman Spectra of Inorganic and Coordination Compounds*, 4th ed., Wiley-Interscience, **1986**.
[26] G. B. Deacon, R. J. Phillips, *Coord. Chem. Rev.* **1980**, *33*, 227.
[27] F. A. Cotton, G. Wilkinson, C. A. Murillo, M. Bochmann, *Advanced Inorganic Chemistry*, 6th ed., Wiley-Interscience, **1999**.
[28] A. W. Addison, T. N. Rao, J. Reedijk, J. van Rijn, G. C. Verschoor, *J. Chem. Soc., Dalton Trans.* **1984**, 1349.
[29] B. Graham, L. Spiccia, G. D. Fallon, M. T. W. Hearn, F. E. Mabbs, B. Moubaraki, K. S. Murray, *J. Chem. Soc., Dalton Trans.* **2001**, 1226.
[30] T. Tokii, N. Watanabe, M. Nakashima, Y. Muto, *Bull. Chem. Soc. Jpn.* **1990**, *63*, 364.
[31] V. M. Rao, D. N. Sathyanarayana, H. Manohar, *J. Chem. Soc., Dalton Trans.* **1983**, *10*, 2167.
[32] M. Merkel, N. Moeller, M. Piacenza, S. Grimme, A. Rompel, B. Krebs, *Chem. Eur. J.* **2005**, *11*, 1201.
[33] A. Elmali, C. T. Zeyrek, Y. Elerman, *J. Mol. Struct.* **2004**, *693*, 225.
[34] P. Gentschev, M. Luken, N. Moller, A. Rompel, B. Krebs, *Inorg. Chem. Commun.* **2001**, *4*, 753.
[35] J. H. Satcher Jr., M. W. Droege, T. J. R. Weakley, R. T. Taylor, *Inorg. Chem.* **1995**, *34*, 3317.
[36] R. Wegner, M. Gottschaldt, H. Gorls, E. G. Jager, D. Klemm, *Chem. Eur. J.* **2001**, *7*, 2143.
[37] P. Basu, B. Katterle, K. K. Andersson, H. Dalton, *J. Biochem.* **2003**, *369*, 417.
[38] B. Katterle, R. I. Gvozdev, N. Abudu, T. Ljones, K. K. Andersson, *J. Biochem.* **2002**, *363*, 677.
[39] M. Fontecave, S. Menage, C. Duboc-Toia, J. M. Vincent, C. Lambeaux, *Biochem. Soc. Trans.* **1997**, *25*, 65.
[40] A. C. Rosenzweig, C. A. Frederick, S. J. Lippard, P. Nordlund, *Nature* **1993**, *366*, 537.
[41] D. A. Whittington, S. J. Lippard, *J. Am. Chem. Soc.* **2001**, *123*, 827.
[42] A. C. Rosenzweig, H. Brandstetter, D. A. Whittington, P. Nordlund, S. J. Lippard, C. A. Frederick, *Proteins: Struct., Funct., Genet.* **1997**, *20*, 141.
[43] B. Graham, G. D. Fallon, M. T. W. Hearn, D. C. R. Hockless, G. Lazarev, L. Spiccia, *Inorg. Chem.* **1997**, *36*, 6366.
[44] B. Graham, M. T. W. Hearn, P. C. Junk, C. M. Kepert, F. E. Mabbs, B. Moubaraki, K. S. Murray, L. Spiccia, *Inorg. Chem.* **2001**, *40*, 1536.
[45] B. DasGupta, C. Katz, T. Israel, M. Watson, L. J. Zompa, *Inorg. Chim. Acta* **1999**, *292*, 172.
[46] T. J. Atkins, *J. Am. Chem. Soc.* **1980**, *102*, 6365–6369.
[47] G. M. Sheldrick, *SHELXL-97* **1997**, University of Göttingen, Germany.
[48] G. M. Sheldrick, *SHELXS-97* **1997**, University of Göttingen, Germany.

Received: May 27, 2008
Published Online: August 12, 2008

